4.0 TSUNAMI MODELLING

Tsunami modelling usually uses a set of mathematical formulae that describe the physical characteristics of tsunami, called a tsunami model, to evaluate and predict the evolution of tsunami waves and their coastal impact. Tsunami models can be used to estimate the probable arrival times of tsunami, their amplitudes, inundation ranges, flow depths and/or current speeds. There are two main types of tsunami models: numerical models (i.e., computer-derived models) and empirical models. Numerical models (i.e., computer-derived simulation packages) use a grid system for the area of interest that contains information such as bathymetry, topography and surface roughness. Using numerical techniques, the numerical models solve the mathematical equations governing the physical process of tsunami wave evolution at each point in the grid system, passing information between surrounding grids. Therefore, a numerical model can incorporate complicated geographic variations in bathymetry, topography and land uses, and can simulate different aspects of tsunami, including their variations in wave amplitude, current speed and inundation depth.

In contrast, empirical models employ statistical relationships, usually calibrated using field observations, to evaluate tsunami properties. It is difficult to incorporate both the changing nature of tsunami waves as they travel, as well as topographical and bathymetrical complexity, in empirical models, but empirical models are very useful for rapid evaluation, particularly when detailed source information and/or high-resolution bathymetric and topographical data are not available. This section provides an overview of current techniques for modelling tsunami, and summarizes tsunami modelling results and what has been learnt from them that is applicable to the New Zealand region.

4.1 NUMERICAL MODELS

Numerical models are used to evaluate and predict the physical characteristics of tsunami. They play an important role for tsunami hazard mitigation in determining arrival times, tsunami heights, current velocities and inundation ranges in a tsunami event, and are especially useful for preparing maps showing inundation and threat levels for potential events along those coastlines vulnerable to tsunami flooding.

Numerical modelling of tsunami allows us to estimate the effects of events which may occur, and to evaluate our understanding of past tsunami. It usually involves three stages:

- Source modelling, in which the generation of the tsunami, either by earthquakes, landslides, volcanic eruptions or bolide impact, is simulated.
- Propagation modelling, in which the dispersal of the tsunami waves around the ocean, sea, or lake is simulated.
- Inundation modelling, in which the water flow over dry land is simulated.

Due to the nature of tsunami evolution, different scales are inevitably involved in tsunami simulations, for example propagation across oceans involves large-scale modelling and land inundation fine-scale modelling. Consequently, tsunami models often have the capability to deal with tsunami evolution at one or more scales.

The devastating 2004 Indian Ocean (Sumatra) tsunami spurred an increase in the development of numerical models. The latest tsunami models simulate tsunami generation, propagation and inundation together, overcoming the difficulty of abrupt changes in conditions at the shore, which is the most dynamic and complex phase of a tsunami. Among others, COMCOT (Cornell University, USA; GNS Science, New Zealand), TSUNAMI-N1/2 (Tohoku University, Japan) and MOST (National Center for Tsunami Research, USA) have demonstrated their capability for the investigation of the three stages of tsunami evolution—generation, propagation and inundation.

Most computer-derived tsunami models, including those aforementioned, were developed by numerically solving Shallow Water Equations (Pedlosky, 1979; Imamura et al., 1988; Vreugdenhil, 1994; Liu et al., 1995; Cho and Yoon, 1998) which neglect the vertical variation of velocity over water depth due to the fact that tsunami wave lengths are usually much larger than ocean depths. Some of the models were derived on the basis of Boussineq-type Equations (Peregrine, 1967; Madsen and Sorensen, 1992; Nwogu, 1993; Kennedy et al., 2000, 2001; Lynett and Liu, 2004a,,b), which include the vertical variation of velocity to some extent, such as CoulWave (Lynett and Liu, 2004a, b) and FunWave (Kennedy et al., 2000, 2001).

At the Institute of Geological and Nuclear Sciences (GNS Science), New Zealand, COMCOT has been continuously under development since the end of 2008, based on the original version from Cornell University, USA (Liu et al., 1998). The latest development incorporates multiple mechanisms for generating tsunami, such as submarine earthquakes and landslides. The built-in fault model is able to model the transient process of rupturing along a fault with variable slip in an earthquake event, which is particularly helpful in evaluating tsunami impacts in nearby coastal areas. Using a nested grid setup, different spatial resolutions may be used for the different stages of tsunami evolution, which allows us to study the entire life-span of a tsunami simultaneously, from its generation in the source area to inundation in coastal regions. This mode has been used to evaluate the tsunami threats to New Zealand for the events of the 2009 M_W8.1 Samoa earthquake, the 2010 M_W8.8 Chilean earthquake and the 2011 M_W9.0 Tohoku earthquake in Japan (see Section 3.3 for more information on these events). It has also been used to study the tsunami hazards and coastal impacts around New Zealand, for both local and distant-source scenarios, for Gisborne District Council (Wang et al., 2009), Tiwai Point (Prasetya et al., 2010a), Riverton (Prasetya et al., 2010b), Auckland Region (Power et al., 2012; Lane et al., 2012), Bay of Plenty and Tauranga.

At National Institute of Water and Atmospheric Research (NIWA), New Zealand, RiCOM (River and Coastal Ocean Model) has been under development for over ten years (Walters et al., 2003, 2005, 2006; Lane et al., 2012) and is frequently used at NIWA, New Zealand for studies of tsunami inundation around New Zealand. It is a general-purpose hydrodynamics and transport model, used to simulate near-shore flooding processes. It uses an unstructured triangular grid with spatially variable resolution allowing high-resolution land grids to be meshed seamlessly with the open ocean for inundation modelling, without the need for nested grids. RiCOM can initialise tsunami using various methods, including static initial conditions (Okada, 1985), a moving bottom boundary (Walters, 1992/2005) and temporally and spatially variable lateral boundary conditions. It has been used to study tsunami hazard and inundations from local, regional and/or distant sources in coastal areas of New Zealand, including Northland, Auckland Region, Waikato, Bay of Plenty, Canterbury and Otago (Lane et al., 2007a/2007b; Arnold et al., 2009; Goff et al., 2006; Walters et al., 2006; Gillibrand et al., 2011; Lane et al., 2012). More recently NIWA has also adapted Gerris, a highly advanced fluid dynamics solver, to enable tsunami modelling, including modules that incorporate tsunami sources and run-up and inundation. Using efficient quad-tree methods, Gerris can adaptively refine its numerical grid where needed to ensure resolution and accuracy. Gerris is very effective at solving for trans-ocean tsunami propagation and run-up (Popinet, 2003). The model has also been used to study potential landslide tsunami hazards in Cook Strait, New Zealand and tsunamis in the Pacific islands, including Wallis and Futuna and Tokelau.

Other numerical models have also been developed, or model applications have been expanded to study the impacts of tsunami. Most of these models are particularly focused on modelling the run-up and inundation, as well as wave propagation close to the source. These models include CoulWave (Cornell University, USA), FunWave (University of Delaware, USA), Tsunami-Claw (Washington University, USA), MIKE21 (DHI, Denmark), and 3DD (ASR Ltd., New Zealand).

4.2 TSUNAMI GENERATION

Tsunami are generated by large-area disturbances on the bottom of a water body, such as submarine earthquakes, landslides and volcanic activity, or on the water surface, for example from meteorite impacts.

4.2.1 Submarine earthquakes

Tsunami source models are well developed for submarine earthquakes, where the seafloor deformation is typically estimated by assuming that the earthquake represents a finite dislocation (i.e., slip) within an elastic body (Okada, 1985; Mansinha and Smylie, 1971). These techniques have been tested against data from numerous real events and generally demonstrate a reasonable agreement, although the 26 December 2004 Indian Ocean earthquake has highlighted some areas for improvement (Lay et al., 2005).

The simple implementation of this type of source model usually assumes a finite rupture interface with uniform dislocation (e.g., slip movement along a fault). Its size and the amount of dislocation may be estimated via empirical relationships based on the seismic magnitude of an earthquake (e.g., Wells and Coppersmith, 1994). This source model is helpful in quickly constructing faulting scenarios and tsunami simulations and generally works well for distant tsunami. However, it neglects the spatial variations in slip, which are very important for evaluating tsunami impacts in regions close to the earthquake source, as demonstrated in the 11 March 2011 Tohoku M_W9.0 earthquake and tsunami. In this event, a slip of over 40.0 metres was estimated around the epicentre and the tsunami produced tremendous damage to the coast areas in Japan from Soma to Miyako, with run-up heights observed of up to 40.0 metres (Fujii et al., 2011; Lay et al., 2011a; 2011b; Mori et al., 2011). In general, the tsunami impact in distant areas is less sensitive to variations in slip.

The Okada (1985) model for fault slip is linear and so a simple improvement is to model a group of fault segments, each with a different amount of slip. Geist (1998) showed that local tsunami run-up can vary by over a factor of 3 depending on the slip distribution. Further model improvements take into account the time of the start of the rupture and the duration of uplift. Variable rupture start time and transient rupture are most important in earthquakes that rupture slowly, such as ‘tsunami earthquakes’ that typically rupture the very shallowest part of the plate interface.

Tsunami earthquakes refer to earthquake events with moderate magnitudes that are nevertheless exceptionally capable of generating tsunami. In these events, tsunami run-up heights are usually much larger than would be expected from their earthquake magnitudes (Kanamori, 1972). This type of earthquake is characterized by a slow rupture velocity and no strong ground shaking. For example, the 15 June 1896 Sanriku Ms 7.2 earthquake in Japan generated an anomalously larger tsunami than expected from its seismic waves. With run-up heights over 25 metres and causing over 22,000 casualties, this became one of the worst tsunami in Japanese history. In the past decades, with implementation of modern seismic detection techniques, more tsunami earthquakes have been identified. They include the 2 September 1992 Nicaragua M_W7.6 earthquake, with run-up heights of over 9.0 m (Kanamori and Kikuchi, 1993; Ide et al., 1993), the 2 June 1994 Java M_W7.6 earthquake, with run-up heights of up to 14 metres and over 250 casualties (Tsuji et al., 1995; Abercrombie et al., 2001), and the 17 July 2006 Java M_W7.8 earthquake, with run-up heights of up to 8 metres and over 600 casualties (Ammon et al., 2006; Fritz et al., 2007).

Historical records show that the east coast of North Island may also suffer from the impacts of tsunami earthquakes. In 1947, two earthquakes, the 25 March 1947 M_W7.1 event and the 17 May 1947 M_W5.9 event, struck offshore from Gisborne and both triggered exceptionally large tsunami. Tsunami heights up to 13 metres were observed along the east coast just north of Gisborne in these events (New Zealand Historical Tsunami Database, by Gaye Downes of GNS Science, in preparation for publication). However, no strong shaking had been felt by local residents (see Sections 3.2 and 5.3.1.2 for further details on these events). Wang et al. (2009) carried out a set of numerical simulations to investigate the tsunami generated by the 25 March 1947 M_W7.1 earthquake. The numerical studies reveal the importance of slip variation and suggest that this event may have been a typical tsunami earthquake (Figure 4.1 and Figure 4.2). Because ground shaking, which is often strongly felt in common earthquakes, will be far less severe in these events, it is difficult to use shaking as a warning to the public of a potential tsunami during this type of event, especially for regions near the earthquake source, such as the east coast of North Island, New Zealand.

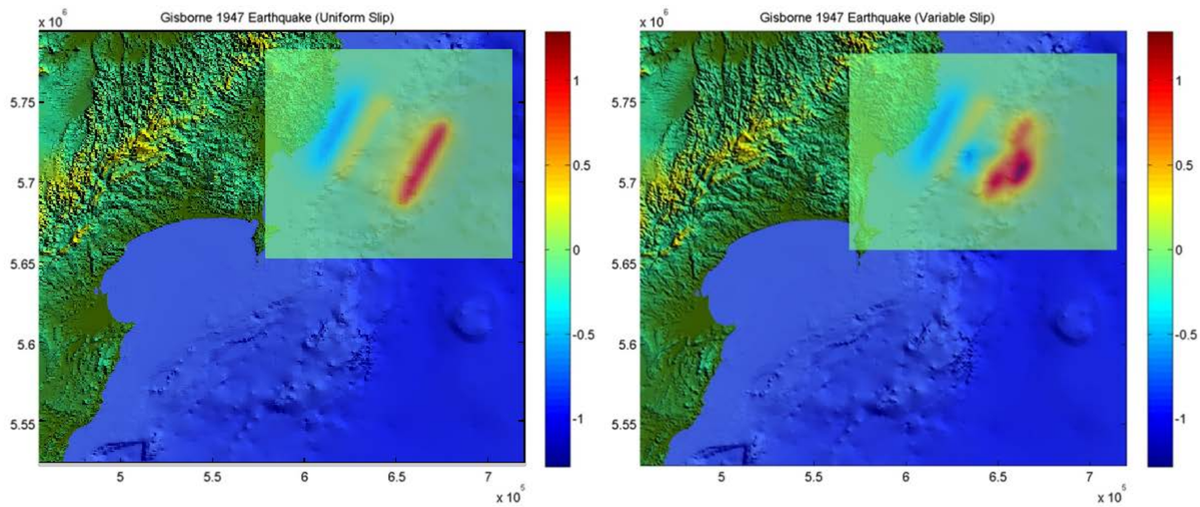

Figure 4.1 Seafloor deformation for the 27 March 1947 Gisborne earthquake (MW7.1) computed using a uniform slip model (left model) and a variable slip model (right panel). The variable slip model assumes that slip is greatest at the site of a subducting seamount (Wang et al., 2009).

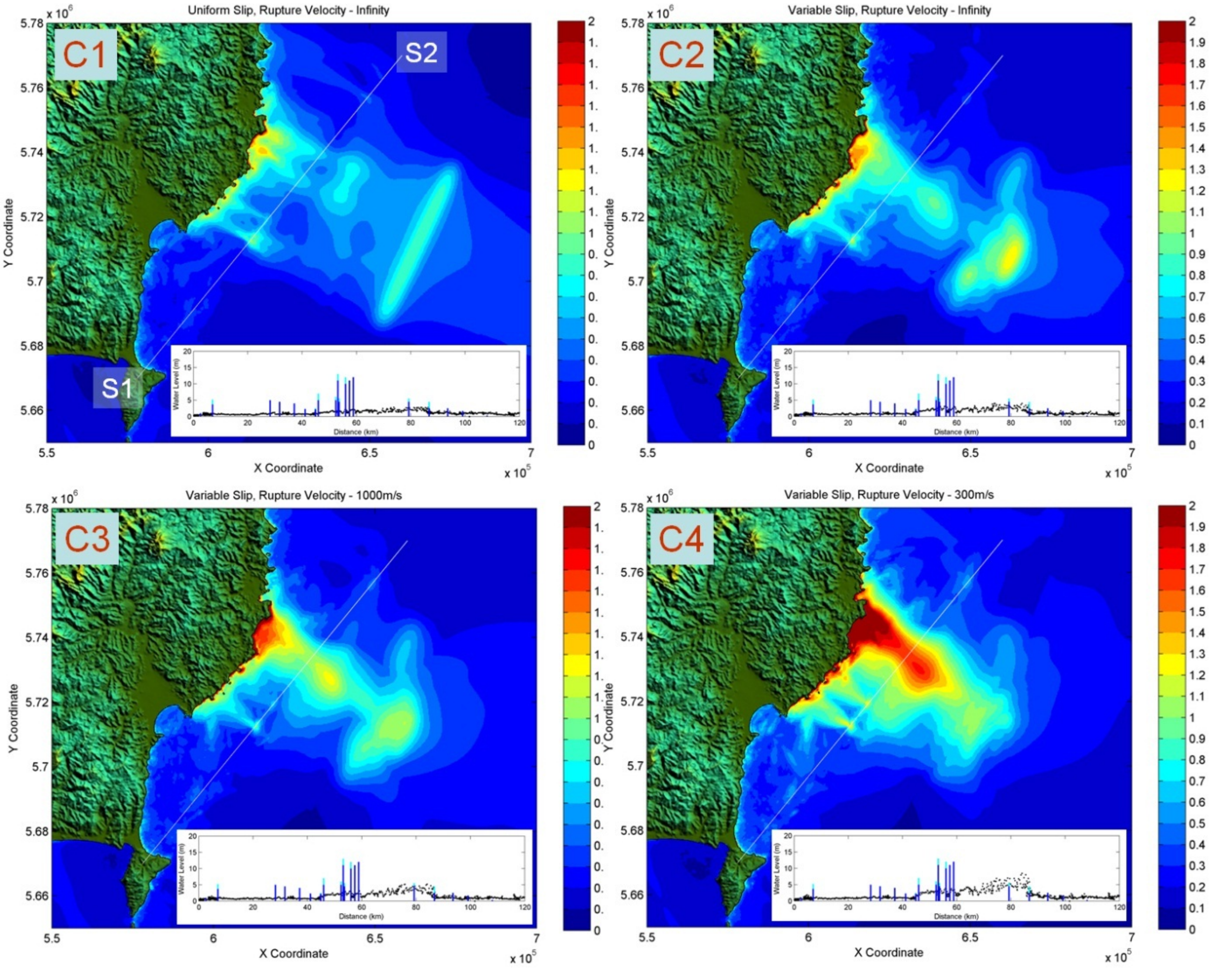

Figure 4.2 The modelled maximum tsunami elevations of the 27 March 1947 offshore Gisborne earthquake (MW7.1). The upper left panel (C1) shows the maximum tsunami elevation derived from a uniform slip model with instantaneous rupture; the upper right panel (C2) shows the maximum tsunami height from a variable slip model with infinite rupture velocity; the lower left panel (C3) shows the maximum tsunami height from a variable slip model with a rupture velocity of 1000 m/s; and the lower right panel (C4) shows the maximum tsunami height from a variable slip model with a rupture velocity of 300 m/s (Wang et al., 2009).

4.2.2 Landslides and volcanoes

Tsunami may also be triggered by landslides or volcanic eruptions. Far less frequent than the occurrences of earthquake tsunami, tsunami generated by landslides and volcanic eruptions may be catastrophic, especially in areas close to the source, but tend to be more localised in impact.

In coastal areas, landslides represent one of the most dangerous mechanisms for tsunami generation, due to their “silent” nature. Moreover, underwater landslides can be triggered by moderate earthquakes and thus the tsunami in such events will be much bigger than expected. Moreover, as they often occur on the continental slope, landslide tsunami offer little time to warn local populations and are particularly challenging for planning evacuation.

Though their role is often controversial, submarine landslides are generally considered to have contributed to the exceptionally large tsunami following several earthquakes, such as the 12 December 1992 Flores Island earthquake in Indonesia, the 17 July 1998 Papua New Guinea M_W7.0 earthquake, with a run-up height of about 15 m and over 2,200 casualties (Geist, 2000; Tappin et al., 2001; Tappin et al., 2008; Synolakis et al., 2002) and the 1 April

1946 Unimak (Aleutian) Ms7.1 earthquake, with run-up heights of up to 42 metres and 167 casualties (Fryer et al., 2004).

The wave amplitudes and characteristics of landslide-generated tsunami have been studied through three main approaches—laboratory experiments, analytical descriptions and numerical simulations (Heinrich, 1992; Watts, 1998; Liu et al., 2005; Enet et al., 2003; Enet and Grilli, 2007). These studies reveal many important aspects of tsunami generated by submarine landslides and indicate that the characteristics of landslide tsunami are related to the shape, physical properties and sliding mechanisms of landslides in a complicated way. Tsunami amplitudes are limited by the volume of mass that moves and the vertical extent of landslide motion (Watts, 1998). Watts et al. (2005) derived semi-empirical predictive equations for tsunami amplitude above the initial location for a two-dimensional rigid landslide. Using mass conservation arguments, they further derived expressions for the characteristic wave amplitude for a 3-dimensional rigid landslide. Experimental studies by Enet and Grilli (2007) validated these empirical models and also indicated that the initial acceleration of landslides is a more important factor in tsunami generation than the terminal velocity. Although empirical relationships can be established for the initial tsunami amplitude generated by simplified rigid landslides, the complexity of deformation, spreading and local bathymetry in reality usually limits their usefulness for more general studies.

Compared to earthquake and landslide tsunami, tsunami generation by volcanic events is far more complicated and often involves more than one physical process. Tsunami can be generated by a variety of volcanic mechanisms—pyroclastic flows, debris avalanches, collapse of sectors of a volcanic edifice, and even by aerial or submarine landslides, and meteo-tsunami caused by the pressure wave from the volcano. Tsunami waves generated by such complex source mechanisms usually behave quite differently to earthquake tsunami. In general, due to the small dimensions of the source areas, these waves are much shorter, with wave periods ranging up to several minutes, and they experience strong dispersion effects. Similar to many landslide-generated tsunamis, their impacts tend to be localized and do not pose a significant danger at great distances from the source (Pararas-Carayannis, 1992; 2002; 2003; 2006).

In brief, for tsunami modelling there are robust, physically based techniques to initialise tsunamis triggered by earthquakes, but none yet for landslides and volcanoes. The generation mechanisms are far more complicated than displacements in earthquake events, and the physics of these mechanisms is in some cases only partly understood. Consequently, while past events can be modelled and specific scenarios for future events can be investigated, the studies are usually on a case-by-case basis and it is harder to develop general insights.

4.3 PROPAGATION MODELLING

In a tsunami event, once the water body has been displaced from its equilibrium position in its source area, the potential energy gained during the generation process is converted to kinetic energy. Tsunami waves are thus generated and spread away from the source area to all the directions. If the tsunami is generated by an earthquake, typically most of the wave energy radiates out along the path perpendicular to the fault line. However, the propagation will be affected by the bathymetry patterns such as submarine ridges, plateaus and seamounts, diverting the propagation direction and focusing tsunami energy in a specific pattern (i.e., wave guiding effect). In ocean basins, the speed at which tsunami waves travel is usually proportional to the square root of the water depth. For example, in the Pacific basin tsunami travel at a speed of 700-900 km per hour, comparable to that of commercial jets. Over continental shelfs, tsunami travel slower than in the deep ocean. However, their amplitude increases as the water depth drops and the propagation will be gradually diverted in a direction perpendicular to the coast line (called shoaling effects).

4.3.1 Modelling tsunami propagation numerically

Simulating tsunami waves spreading out from the source is well understood in terms of the underlying physics. Below we present two examples using COMCOT to model the propagations of the 27 February 2010 Chile M_W8.8 event and the 11 March 2011 Tohoku M_W9.0 event in Japan (see Section 3.3 for more information on these events).

In the 27 February 2010 Chile tsunami, the major energy of the tsunami was steered toward Japan and the Kuril Islands (Figure 4.3 and Figure 4.4). New Zealand was off the main track of its impact. However, the Chatham Rise, together with the Campbell Plateau, east of the South Island, served as a wave guide, focusing more energy toward the east coast of South Island (Figure 4.3). In New Zealand, the first peak of the tsunami arrived at Chatham Island about 12 hours after the earthquake, with increases in water level of up to one metre recorded at tsunami gauges in Chatham Island and Gisborne. The sea levels oscillated for over 12 hours before they attenuated.

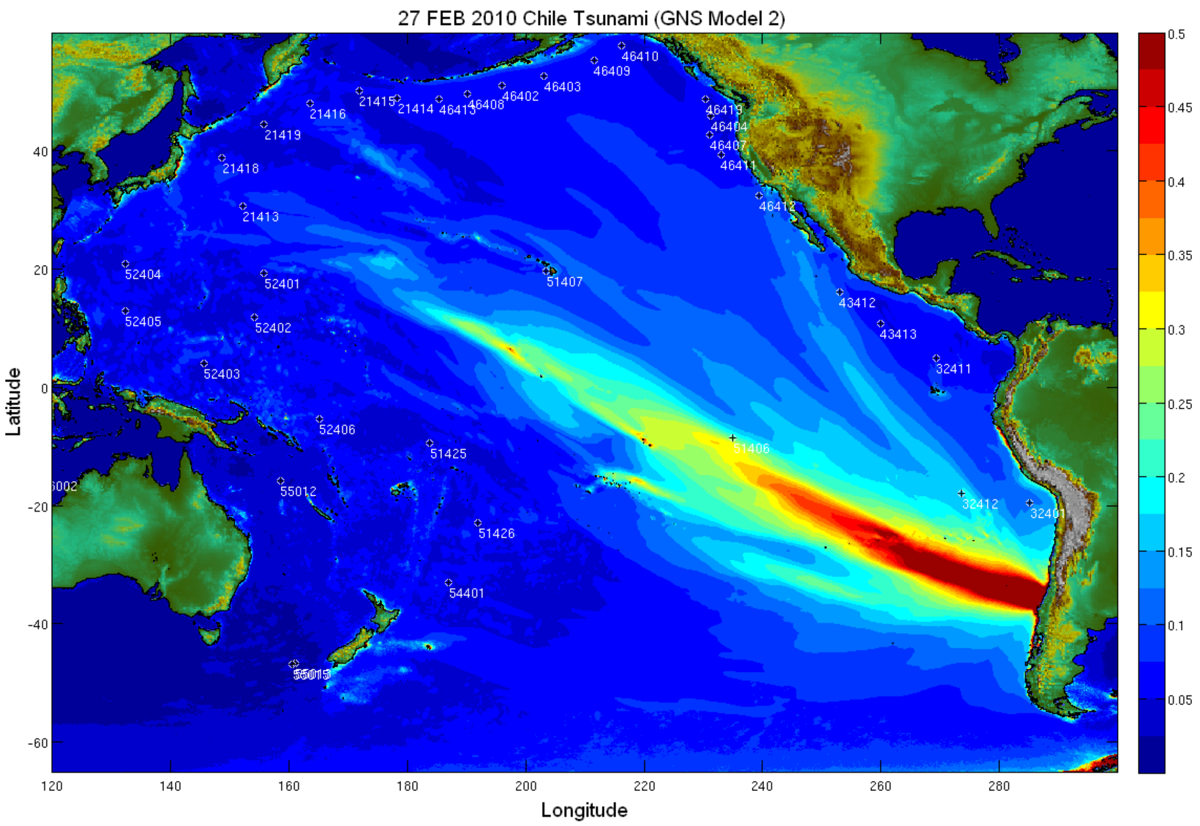

Figure 4.3 Modelled distribution of maximum tsunami elevations throughout the Pacific for the 2010 Chilean tsunami event (numerical simulations by tsunami scientists at GNS Science, New Zealand). DART buoys are indicated by white circles with a black cross inside. The colour scale presents tsunami elevations above ambient water level in metres.

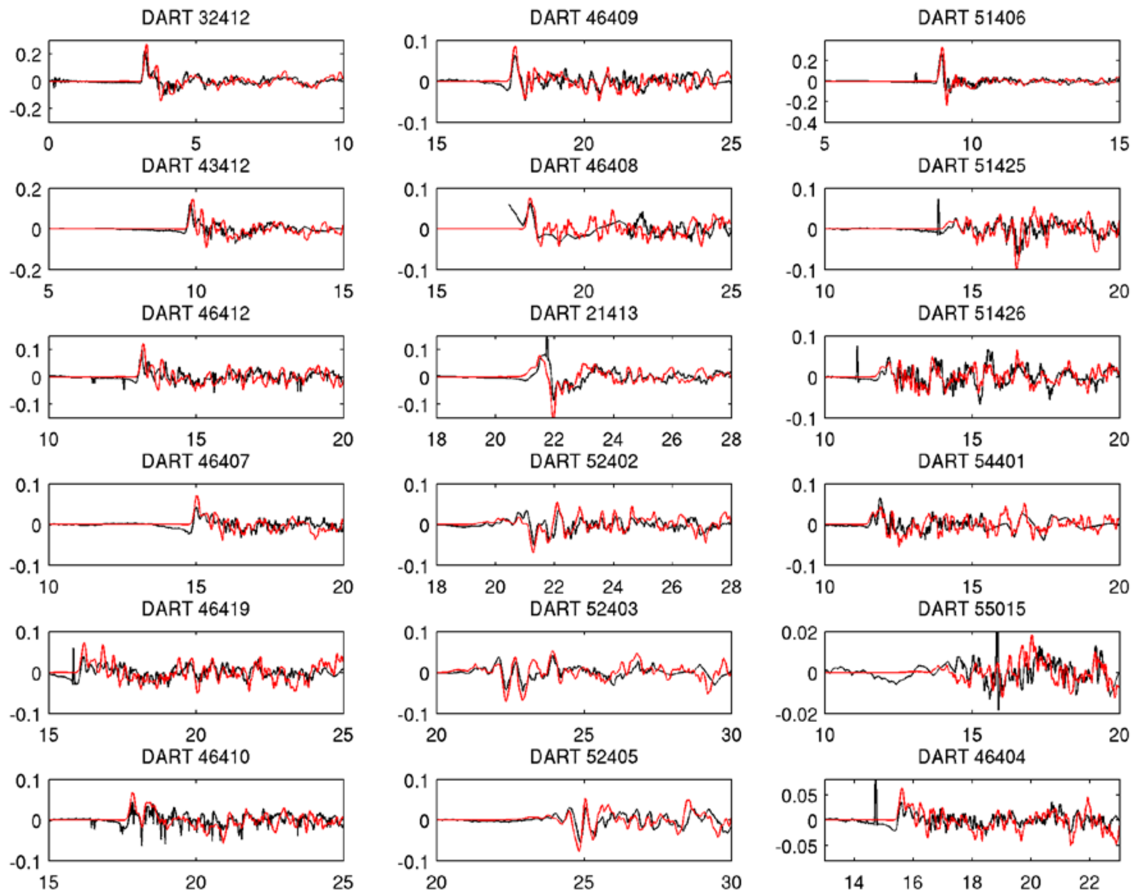

Figure 4.4 Comparisons between the modelled sea surface fluctuations and the measurements at DART buoys for the 2010 Chilean tsunami (numerical simulations by tsunami scientists at GNS Science, New Zealand). The red colour presents the modelled data and the black colour indicates the measurements. The horizontal axes show hours after the main shock and the vertical axes denote the sea-level anomaly in metres.

In the 11 March 2011 Tohoku M_W9.0 earthquake in Japan, numerical simulation shows that the major energy of the tsunami propagated toward the coast of North and South America through Hawaii (Figure 4.5 and Figure 4.6). The minor amount of tsunami energy travelling toward New Zealand was mostly blocked by Pacific islands, such as Solomon Island, Tonga, and Fiji (Figure 4.5). In New Zealand, the tsunami started to affect the North Island about 12 hours after the main shock. Figure 4.6 shows a comparison between modelled and measured sea level fluctuations during this tsunami. Tsunami amplitudes of up to 1.0 metre were recorded by several tsunami gauges at the coasts of New Zealand, however, the sea level oscillations lasted for over 30 hours before they attenuated (Figure 4.7). This indicates that people in coastal areas of New Zealand need to remain vigilant for long periods of time following tsunami from distant source locations.

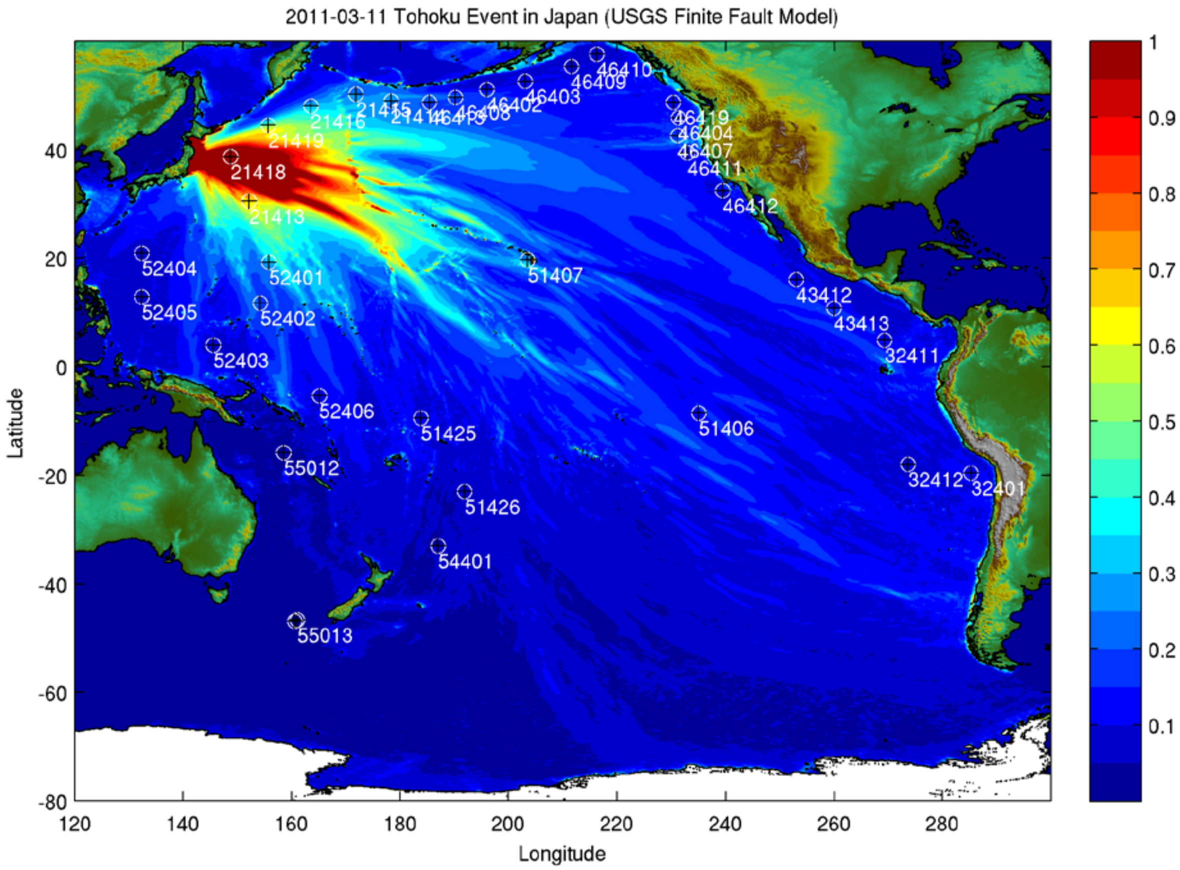

Figure 4.5 Modelled maximum tsunami elevations in the Pacific for the 11 March 2011 Tohoku earthquake in Japan (tsunami simulations were carried out by tsunami scientists at GNS Science, New Zealand, using COMCOT, with the source model of the USGS finite fault solution). DART buoys are indicated by white circles with black crosses inside. The colour scale represents maximum water level increments in metres due to this

tsunami.

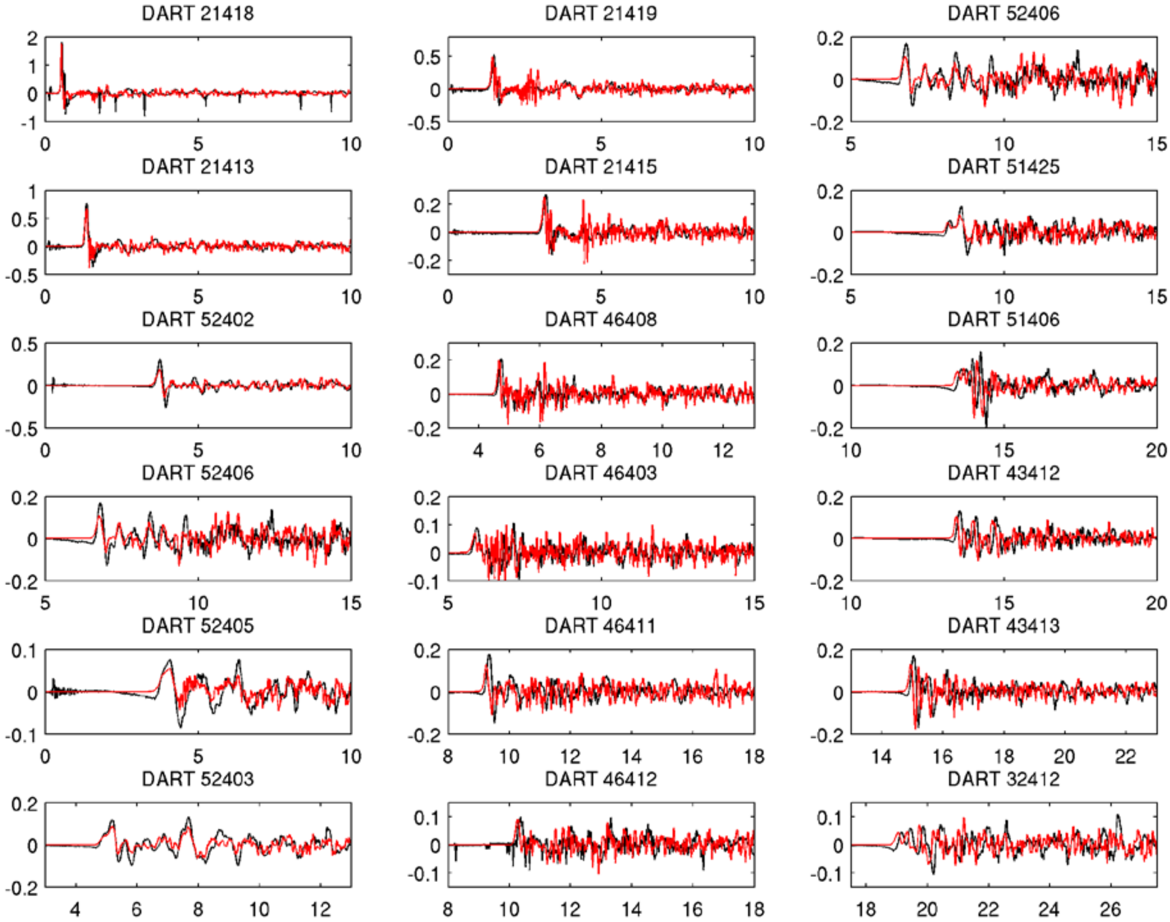

Figure 4.6 Comparison between the tsunami sea-level fluctuations over time derived from modelling and the measurements made at DART buoys (filtered) throughout the Pacific for the 2011 Tohoku event in Japan. The red colour presents the modelled data and the black colour indicates the measurements. The horizontal axes show hours after the main shock and the vertical axes denote the sea level anomaly in metres.

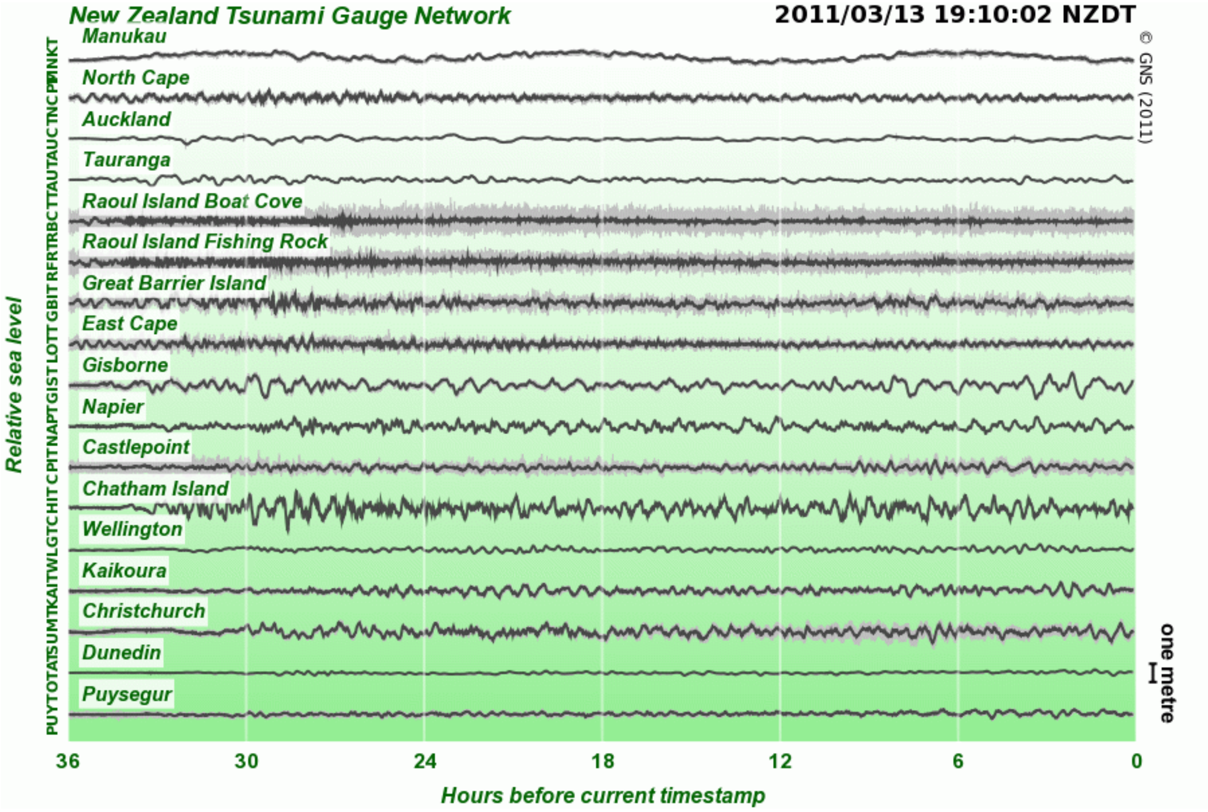

Figure 4.7 Measurements of the 11 March 2011 (UTC) Japan tsunami at coastal tsunami gauges in New Zealand. The measurements at Gisborne and Chatham Island show that significant oscillations were still being recorded over 30 hours after the leading wave arrived.

4.3.2 Insights from propagation modelling

Extensive studies and numerical modelling have been carried out to evaluate tsunami hazards in New Zealand from local, regional and distant sources (see examples in Figure 4.1 and Figure 4.2, Figure 4.8 and Figure 4.9 and studies listed in Appendix 1). Many useful insights can be gained from the propagation modelling and these are summarized below.

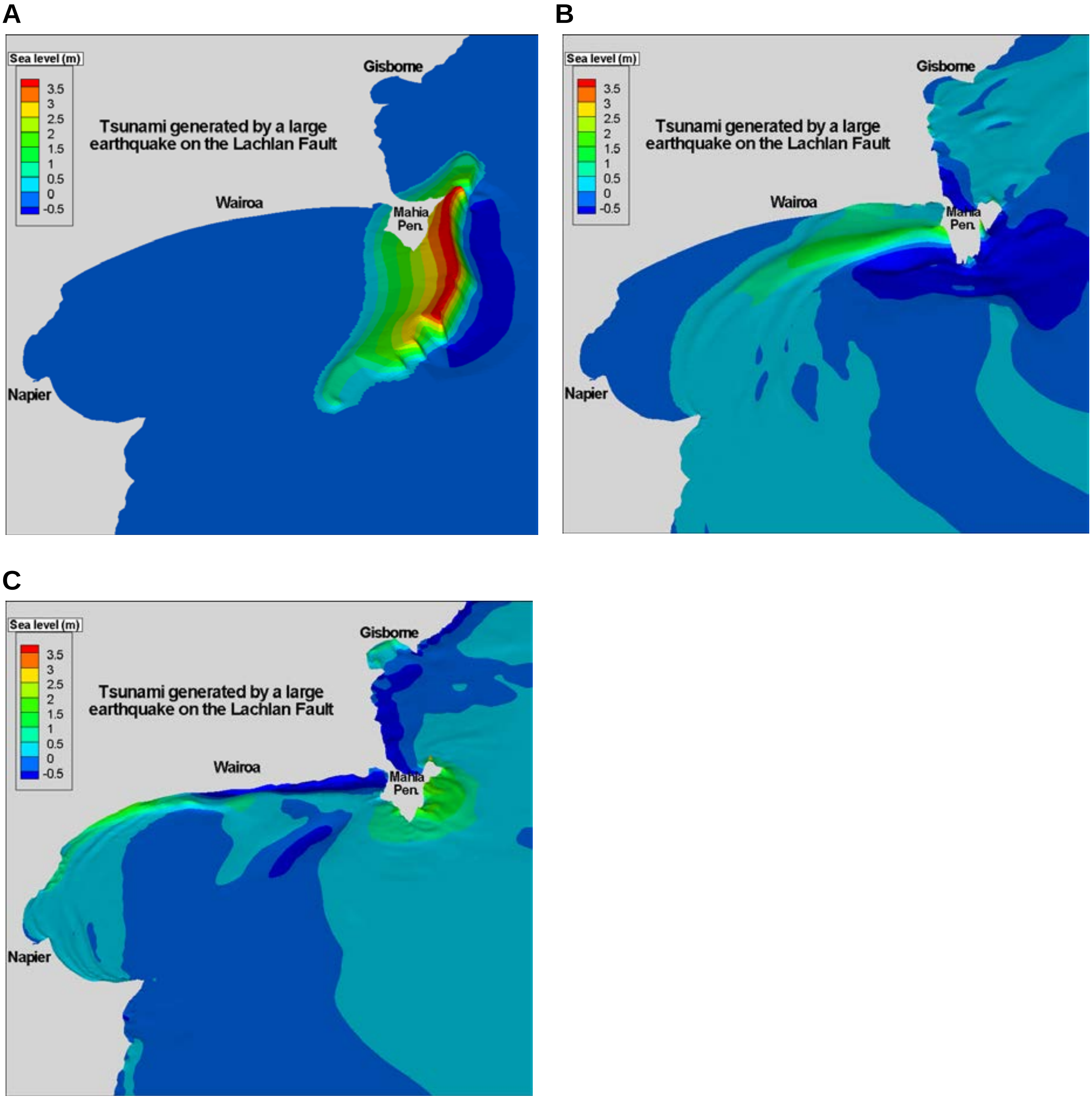

Figure 4.8 A series of images illustrating the propagation of a tsunami generated by an earthquake on the Lachlan fault (which lies offshore of Hawke's Bay, approximately at the position of the tsunami in image A), modelled by Roy Walters et al. with RiCOM model at NIWA, prepared for the Hawke's Bay Aquarium.

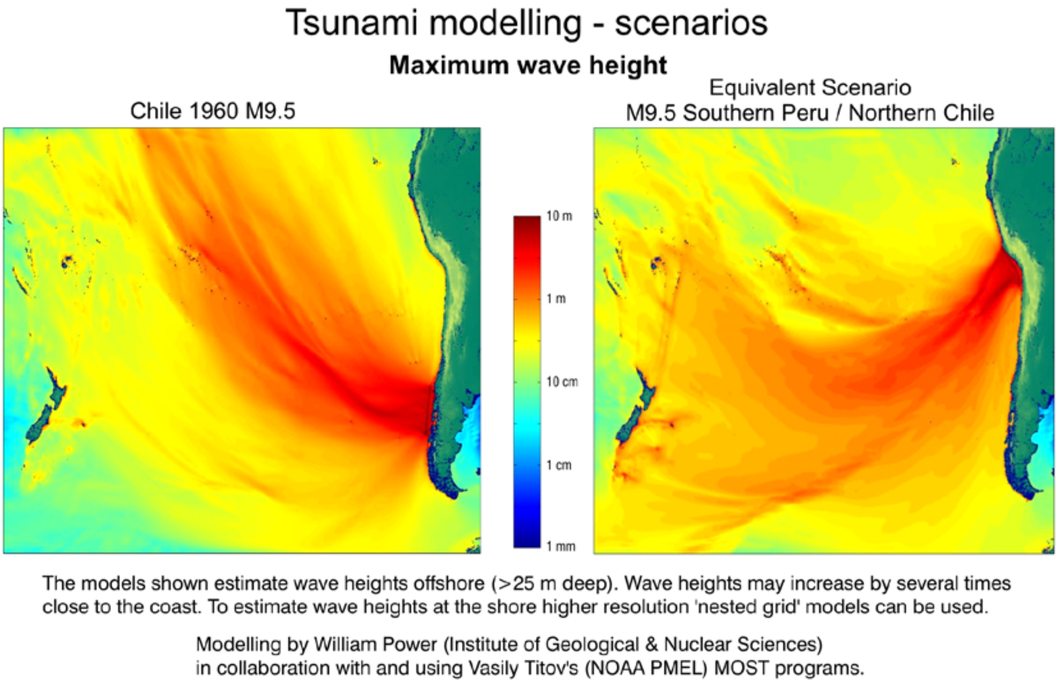

Figure 4.9 A comparison of two scenarios for South American tsunami affecting New Zealand, illustrating the effect that directivity of the source can have on distant locations. This effect explains why the ~M9 1868 Peru earthquake caused tsunami heights in New Zealand that were about as large, and in some locations larger, than those caused by the ~M9.5 1960 Chile earthquake, even though the 1960 earthquake was substantially greater in magnitude (see Section 3.2).

- Earthquake-generated tsunami typically propagate in such a way that most of the wave energy is directed perpendicular to the fault on which the earthquake occurred, and the initial wave is separated into two components travelling in opposite directions.
- Landslide sources can be highly directional, sending a fairly concentrated tsunami 'beam' perpendicular to the slope which has given way and in the direction of the landslide movement (Ward, 2001; Walters et al., 2006). Many volcano sources can also be highly directional, but more typically radiate in a circular pattern.
- Where the dimensions of the tsunami source are small, less than a few tens of kilometres, the resulting waves are subject to dispersion, in which the different frequencies present in the tsunami wave propagate at different speeds. This leads to a stretching-out of the tsunami wave train, and generally lower wave amplitudes. This is one reason why landslides and volcanoes tend not to be a tsunami risk at large distances from the source.
- Tsunami waves tend to become concentrated above undersea ridges because of refraction. In this situation the ridge acts as a 'waveguide', which can lead to enhanced tsunami wave heights at locations where these ridges lead to the shore (Koshimura et al., 2001). In New Zealand a good example is given by the Chatham Rise, an area of shallow bathymetry which lies between Banks Peninsula and the Chatham Islands. The presence of this ridge leads to larger wave heights reaching Banks Peninsula than would otherwise be the case.

- Bays and inlets around the coast have specific natural frequencies, determined by the time it takes for water to slosh into and out of the bay (e.g., Walters, 2002; Walters and Goff, 2003; Tolkova and Power, 2011). If the natural frequency of a bay matches that of the tsunami waves then the waves may be amplified. This can often explain variations in tsunami height that may at first appear random along a given section of coastline. Identifying the natural frequencies of coastal bays and comparing them with characteristic frequencies for tsunami is a useful first step towards identifying those areas most at risk.

Specific aspects of tsunami that affect New Zealand

- Of the South American tsunami sources, it is those lying between the Peru-Chile border (19°S) and the 8°S line of latitude, which are most effective at directing tsunami towards New Zealand. The tsunami of 1868, which was the worst distant-source tsunami of historical times in this country, originated from the southern half of this region (about 17.7°S). The last large tsunami from the northern half of this region (about 12.5°S) was in 1746, too early to appear in written records in New Zealand, but modelling suggests that such tsunami are likely to also have a strong impact here. Locations on the east coast of New Zealand tend to be the most vulnerable to South American tsunami, but the ability of tsunami to bend around corners in the coastline means that they can still pose a hazard to locations that are out of direct line-of-sight (Figure 4.9).
- Distant tsunami originating from locations in the Northern hemisphere, such as Cascadia, and the Aleutians, and also from areas of the southwest Pacific north of New Zealand, tend to have their greatest impact on Northland, the Coromandel, and the Bay of Plenty.
- Local tsunami generated by submarine landslides and thrust faults can have a large local impact on the east coast of New Zealand from south of Kaikoura northwards to Northland.
- The east coast of North Island may have suffered from tsunami earthquakes. Modelling studies suggest the 27 March 1947 M_W7.1 earthquake and the 17 May 1947 M_W6.9 earthquake offshore from Gisborne were tsunami earthquakes that generated far larger tsunami than expected given the magnitude of the earthquakes. This type of earthquake is usually not associated with strong ground shaking.
- As observed from the recent 2010 Chilean tsunami and the 2011 Japan tsunami, coastal oscillations tend to last for a significant duration. In the 2011 Japan tsunami, in Gisborne and Chatham Island (among others), coastal tsunami gauge records show that the coastal water levels had oscillated for over 30 hours before apparent decay occurred (Figure 4.7).

Numerical modelling studies relevant to New Zealand are tabulated in Appendix 1.

4.4 INUNDATION MODELLING

Inundation modelling is used to determine the range of flooding inland and the flow depths in a tsunami event. There are various methods by which inundation can be modelled; in order of increasing complexity and accuracy these are:

- A simple bathtub model that projects the level of the maximum tsunami height inland;
- A rule-based tsunami height attenuation model, applied inland from the coast. This approach derives a more realistic output than a simple ‘bathtub’ model but is still a rough estimate that cannot account for physical variations in wave behaviour.
- A computer-derived simulation model that allows for added complexities such as varying land roughness depending on land use and evaluates comprehensive dynamics of tsunami waves, but which still takes as input a single tsunami height at the coast.
- A computer simulation that takes account the physical properties affected by land use and the dynamics of the tsunami waves, but which is directly linked to a tsunami propagation model. This provides the most comprehensive inputs to the inundation modelling.

4.4.1 Numerical modelling of tsunami inundation

In a tsunami event, or scenario study with a specified source model, inundation in a specific area can be modelled numerically, provided high-resolution topography and bathymetry data are available. While a tsunami may travel thousands of kilometres across ocean basins, land inundation is confined to tens to hundreds of metres (a few kilometres in extreme cases). To accurately model this requires an inundation grid that can resolve these scales. The inundation grid covers not only the sea but also land areas of interest. The depth and velocity of the water in wet areas are modelled using standard physical equations (e.g., non-linear shallow water equations or Boussinesq-type equations) and a wetting/drying algorithm determines the instantaneous boundary of the water, allowing the wave to inundate the land areas but also for areas to become dry as the wave retreats. The inundation modelling must be linked to a propagation model, which provides sea surface fluctuations and velocity information to the inundation model as boundary conditions.

COMCOT uses a series of nested grids to increase resolution in areas where inundation modelling is required (Wang and Power, 2011), passing information from the larger scale propagation grids on the boundaries of the more refined grid. RiCOM uses an unstructured grid which can be gradually refined for areas of interest, allowing a seamless transition between propagation and inundation. Gerris uses adaptive grid-refinement techniques to increase resolution where and when inundation occurs.

Numerical models provide the inundation range, flow depth and velocity information for a tsunami simulation. Together with maps or aerial photos, these data can be used for tsunami hazard planning, such as evaluation of potential tsunami hazards, development of evacuation maps, etc. The magnitude of the forces impacting structures in the inundated areas may also be evaluated using the results of inundation modelling, to provide guidance on building tsunami-resilient communities (Wang and Liu, 2007; Wijetunge et al., 2008). Figure 4.10 and Figure 4.11 show the modelled flow depth in the Gisborne area for an M_W9.0 scenario event, involving rupture of the whole Hikurangi subduction margin off the east coast of New Zealand. In these figures, the modelled flow depth is overlaid on a Google map and on an aerial photo of the same area to illustrate the extent of inundation (Wang et al., 2009).

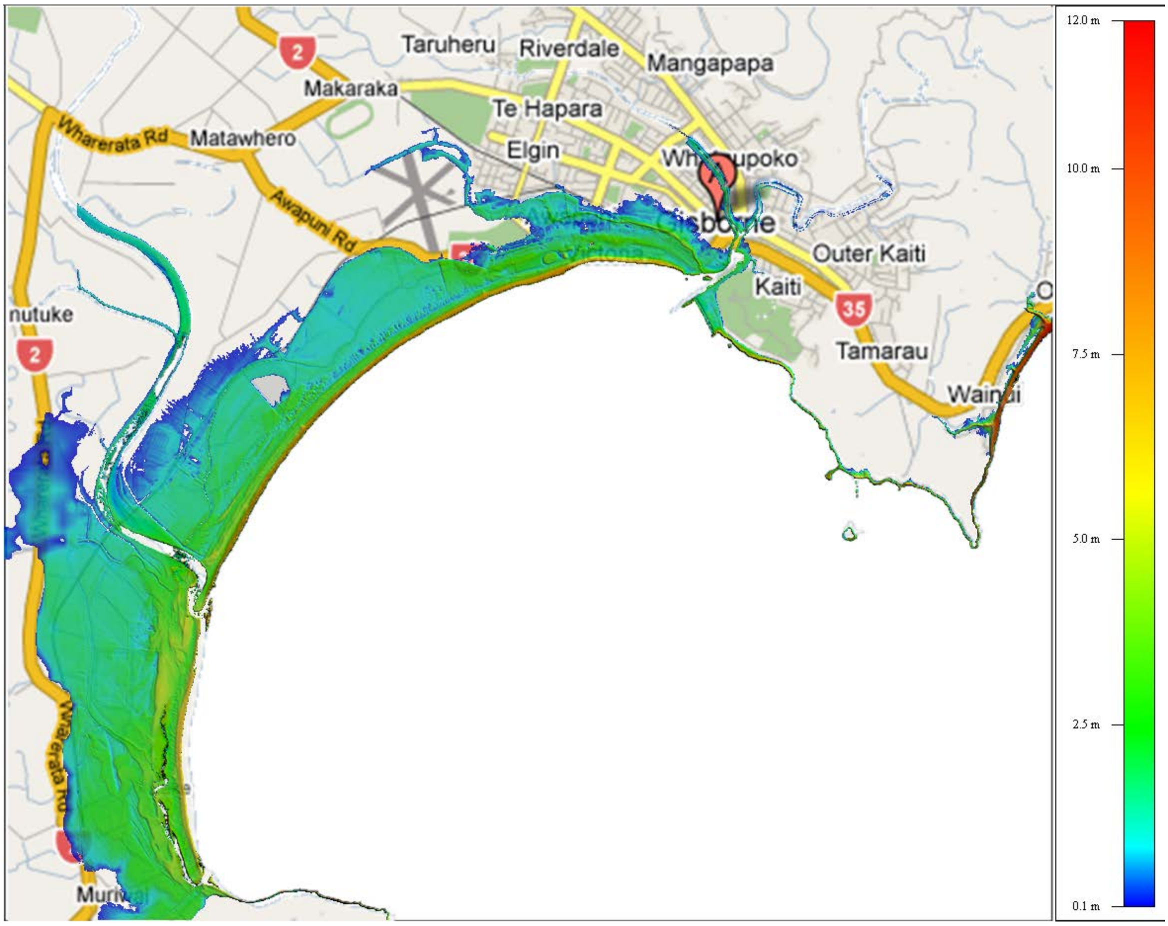

Figure 4.10 The modelled flow depth in the Gisborne area for an MW9.0 scenario event involving rupture of the whole Hikurangi margin. The numerical simulation was performed by Wang et al. (2009) using the COMCOT model and the modelled flow depth on land is overlaid on a Google map).

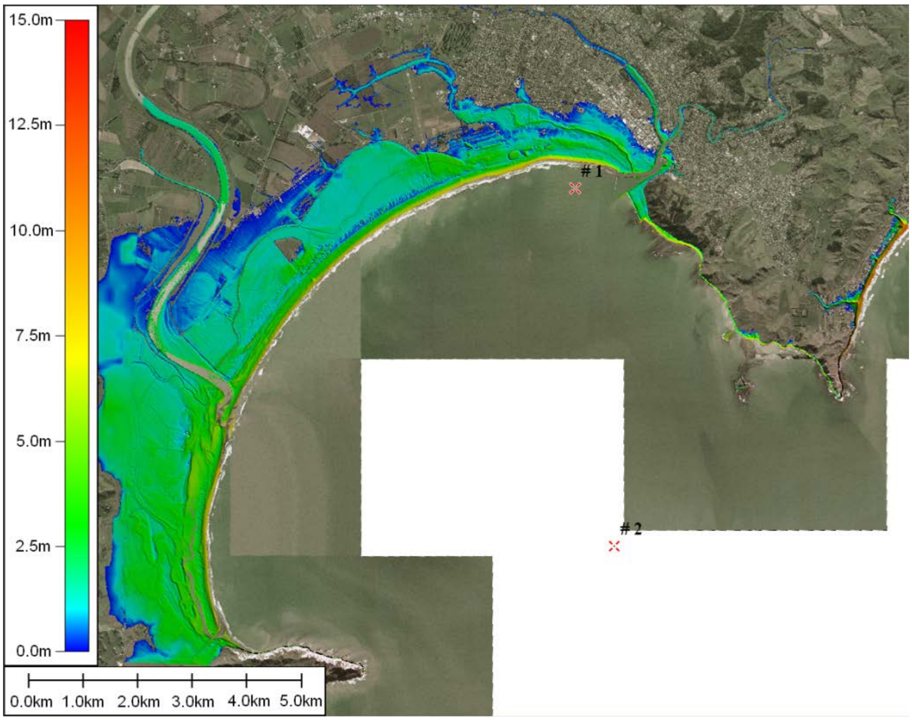

Figure 4.11 The modelled flow depth in Gisborne area for an MW9.0 scenario event involving rupture of the whole Hikurangi margin. The numerical simulation was performed by Wang et al. (2009) using the COMCOT model, and the modelled flow depth on land is overlaid on an aerial photo. The red crosses indicate the location of virtual tidal gauges for time history data output.

High-resolution data on topography is necessary to produce a satisfactory output for inundation modelling. This type of data usually comes from LiDAR or RTK surveys. LiDAR (Light Detection and Ranging) is an optical remote-sensing technology that can be used to measure the distance to the land surface from an aircraft by illuminating the target with light, e.g., a laser, and thus create high-resolution topography data with vertical accuracy usually in the 10-15 centimetre range. RTK (Real-Time Kinematic) survey is a technique used in land survey based on the use of carrier phase measurements of GPS or GLONASS signals, where a single reference station provides the real-time corrections with up to centimetre-level accuracy. RTK surveys, while very accurate, are very labour intensive and have limited spatial extent. They are useful to delineate specific features (such as stopbanks) or locate damaged buildings or indicate inundation extents in post-disaster surveys. If LiDAR or some other high-resolution DEM is not available, results from RTK surveys may be used to build up a rough topographic model.

As one of the factors that retard inundation, land-use conditions also have to be considered and are usually incorporated into the modelling process as land roughness. LiDAR information can also be used to derive roughness estimates for inundation modelling (Smart et al., 2004).

4.5 EMPIRICAL TSUNAMI MODELLING

An alternative to directly modelling the physical processes in a tsunami is to use historical data to construct a statistical model of probable tsunami characteristics (e.g., height at the coast) as a result of factors such as earthquake magnitude and distance to the epicentre. These models are very quick to compute, but because they bypass physical considerations by statistically fitting the data to a simple equation, they are limited in their ability to predict tsunami characteristics, e.g., tsunami heights and inundation extents, in a relatively simple situation.

4.5.1 Empirical modelling of tsunami heights

4.5.1.1 Estimating heights of tsunami from distant sources

Based on a compilation of historic data, largely for the Pacific Ocean, Abe (1979) proposed the following equation for estimating the tsunami height, H, of a tsunami at a distant shore due to an earthquake of magnitude M_W

$$H = 10^{(M_W - B)} \qquad \textbf{Equation 4.1}$$

Where B is a parameter that varies for each site and earthquake source. B can be determined using either historical data, or numerical modelling, or a combination of both. The data on which Abe (1979) based this equation has considerable scatter, so the relationship has significant uncertainty which must be taken into account.

Tsunami-height information from historical observations, or from a collection of synthetic models, can be used to estimate parameter B for each site and source region. In Section 6 we apply this method using synthetic models to estimate B, an approach which is sometimes referred to as semi-empirical modelling.

4.5.1.2 Estimating heights of tsunami from local sources

For local source tsunami, the equivalent Abe relationship to that used for distant sources is given by:

$$Ht = 10^{M_W - \log R + 5.55 + C} \qquad \textbf{Equation 4.2}$$

where H_t is the tsunami height at a local coast, *R* is the source-to-site distance and *C* is a parameter that varies for each site and earthquake source. The best available values of *C* are derived from Japanese data and have possible values of 0.0 and 0.2, depending upon location. Because Ht in Equation 4.2 becomes unrealistically large at small values of R, Abe introduced a limiting tsunami height near the source of:

$$Hr = 10^{0.5M_W - 3.30 + C} \qquad \textbf{Equation 4.3}$$

These equations estimate the tsunami height based only on earthquake magnitude and distance, and take no account of the effects of bathymetry or source orientation, consequently it is important to take into account the uncertainty in these estimates. More details of this analysis, including the uncertainty treatment, are given in Section 6. The interpretation of Ht needs further comment—originally it was interpreted, and the equation parameters used, were in terms of peak-to-trough tide gauge measurements. However direct interpretation of these results is complicated by the limitations of tide gauges at the time the data was collected—these often tended to underestimate wave heights (Satake et al., 1988). Abe (1995) later related Ht to the average run-up height along a section of coast, and 2Ht to the maximum run-up height anywhere along a section of coast (see Kajiura, 1983 and Abe, 1995 for details); this is the interpretation used in Section 6.

4.5.2 Empirical modelling of tsunami inundation

Empirical inundation modelling is usually used for areas where numerical modelling is at a preliminary stage because resources and data are limited. There are many different processes taking place during inundation, some of which may not be well understood. Consequently, effective modelling of the combined processes remains challenging. In addition, high-resolution numerical modelling is time-consuming and requires substantial computing capacity. As an alternative, empirical models can provide rapid estimates when they are needed.

The 2005 Tsunami Hazard and Risk Report described several empirical modelling approaches to tsunami inundation. Since 2005, one approach has often been used for interim evacuation zone planning in situations where data and computing resources were not yet available for full modelling. Due to the conservative assumptions used, it is more accurate to describe this as an ‘evacuation zone estimation method’ rather than a ‘tsunami inundation model’. This method is briefly explained in the following section.

4.5.3 Deriving rules for defining tsunami evacuation zones

Field surveys following tsunami have involved collection of a lot of data on tsunami flow-heights and run-up heights for several events (e.g., the 2004 Indian Ocean tsunami). Analysis of comprehensive survey data from large tsunami shows that the largest run-up heights occur close to the coast, while the inundation extends furthest inland in areas of low, flat topography.

Field survey data from Lhok Nga and Banda Aceh (Lavigne et al., 2009) shows this relationship (Figure 4.12) in measurements of the 2004 Indian Ocean tsunami. Note that this data was collected onshore from sections of coast ~10-20km long, i.e., it does not represent just a single transect. From this data it is possible to define an 'envelope' which sets the maximum possible water level at a given distance from the coast. Assuming a linear envelope, we find that the maximum achievable water level decreases by approximately 1 metre for every 200 metres inland.

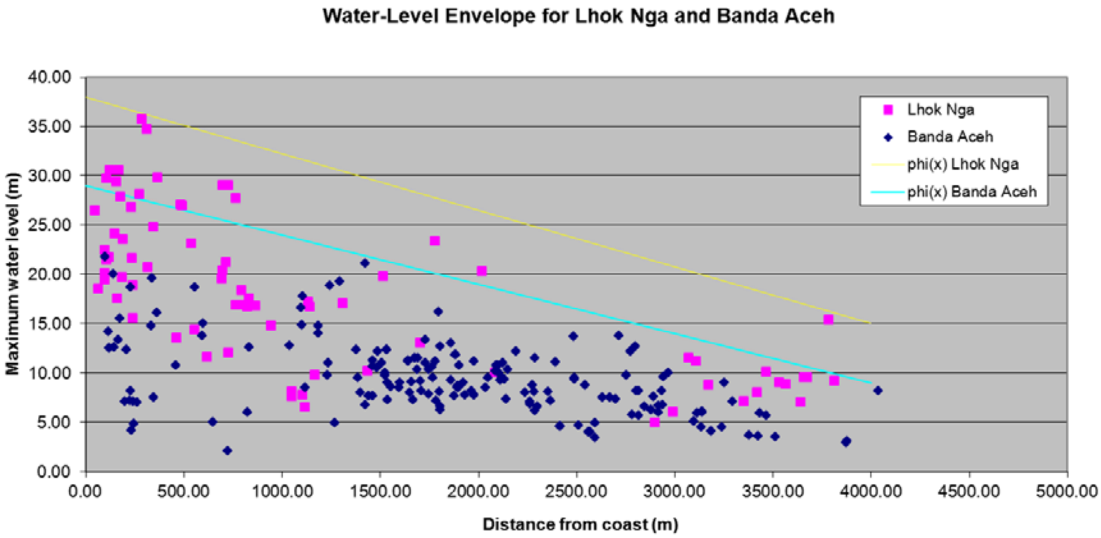

Figure 4.12 Water level plotted as a function of distance from the coast, using field survey data from the districts of Lhok Nga and Banda Aceh, as recorded by Lavigne et al. (2009) following the 2004 Indian Ocean tsunami.

This analysis of survey data is valid only if the dataset of survey points is comprehensive and if the tsunami encounters varied terrain (i.e., with various slopes and topographic forms). Unfortunately, these conditions are rarely met—of the datasets in Figure 4.12 Lhok Nga covers quite a variety of terrain, whereas in the area spanned by the Banda Aceh data the terrain is more uniform. The 2011 Japan tsunami has provided excellent datasets for more analyses of this type (Fraser and Power, 2013). Smaller tsunami are rarely field surveyed in as much detail; one exception is the 1983 Japan Sea tsunami, for which the maximum achievable water level dropped off faster, approximately 1 metre for every 100 metres inland, as might be expected from a shorter period tsunami from a smaller source.

Using the empirical rule to define evacuation zones then requires an estimate of the maximum possible water level at the coast, and then including in the zone those points that lie inside the 'wedge' defined by the 1:200 rule. The method is applied conservatively—the maximum height at the coast is usually taken to be twice the water level at the coast of a tsunami propagation model with reflecting 'wall' boundary conditions (i.e., assuming that small-scale topographic features can at most double the tsunami height), and the 1:200 decay is taken as a conservative limit on the decay rate.

Tsunami propagate further along rivers than they do across land. Data from Banda Aceh suggests they may travel about twice as far, hence a 1:400 decay (a 1 metre drop for every 400 metres upriver) is generally assumed.

Fraser and Power (2012) compared tsunami evacuation zones defined using the above rule, and assuming a 35 m maximum run-up at the coast, with actual inundation data from the 2011 Japan tsunami. They found the resulting zones to be successful in encompassing the true extent of inundation, with a degree of over-evacuation that was acceptable for a simple interim evacuation mapping technique.

4.5.3.1 Limitations of empirical inundation modelling and rule-based evacuation zoning

The rule-based approach to evacuation mapping has been applied as an interim measure where data and computing resources are limited. It has been designed conservatively, as explained above; however this conservatism comes at a cost—it may result in evacuating larger areas than necessary. It is anticipated that such rule-based evacuation zoning will be phased out as the data and computational needs for full numerical modelling become available.

4.6 REAL-TIME TSUNAMI MODELLING AND FORECASTS

Numerical models are extremely helpful for studying the tsunami impacts of historical events, and for evaluating the tsunami threat from potential events, or establishing a tsunami scenario database. However, it can be very challenging to apply them to evaluating and forecasting tsunami threats in real time, especially for tsunami from local or regional sources, due to the extensive time required for model setup, computation and data analysis.

Emergency managers and other officials are in urgent need of operational tools that will provide accurate tsunami forecasts to guide them in making rapid, critical decisions in which lives and property are at stake. In light of this, advanced tools have been developed to evaluate and forecast tsunami threats in real time. In the USA, a next-generation real-time tsunami forecast model has been developed by the National Oceanic and Atmospheric Administration (NOAA) Center of Tsunami Research (NCTR). The model, Web-based Short-term Inundation Forecast of Tsunami (WebSIFT), can provide real-time deep-ocean tsunami propagation forecast worldwide (Titov et al., 2005; Gica et al., 2008). This model uses a pre-computed propagation database of tsunami evolution based on unit earthquakes from fault planes with a size of 100 km x 50 km called unit sources. These unit sources, with a slip amount of 1.0 metres, are placed along the subduction zones around the rim of ocean basins. Then the propagation database is constructed by running a propagation model to obtain offshore scenario wave kinematics for each unit source. In a specific event, the deep-ocean tsunami propagation can be quickly obtained through the linear combination of unit sources using an inverse analysis in which real-time tsunami measurements from DART (Deep-ocean Assessment and Reporting of Tsunamis) are used to improve the tsunami forecast. The DART system is particularly designed to detect tsunami waves and provide real-time measurements of sea-level changes due to tsunami (Figure 4.13).

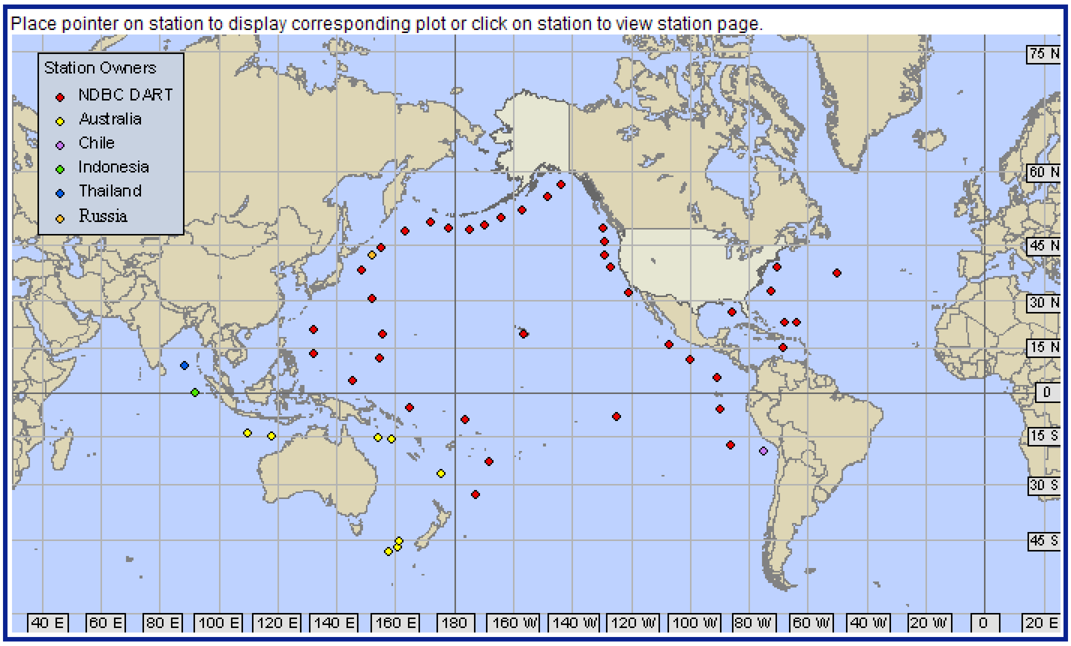

Figure 4.13 DART buoys in deep oceans (NCTR, USA). At DART buoys, sea levels are measured by bottom pressure recorders and transmitted to related data centers in real time.

Figure 4.14 shows the user interface of WebSIFT and the forecasted tsunami amplitude and arrival time for the 29 September 2009 Samoa event.

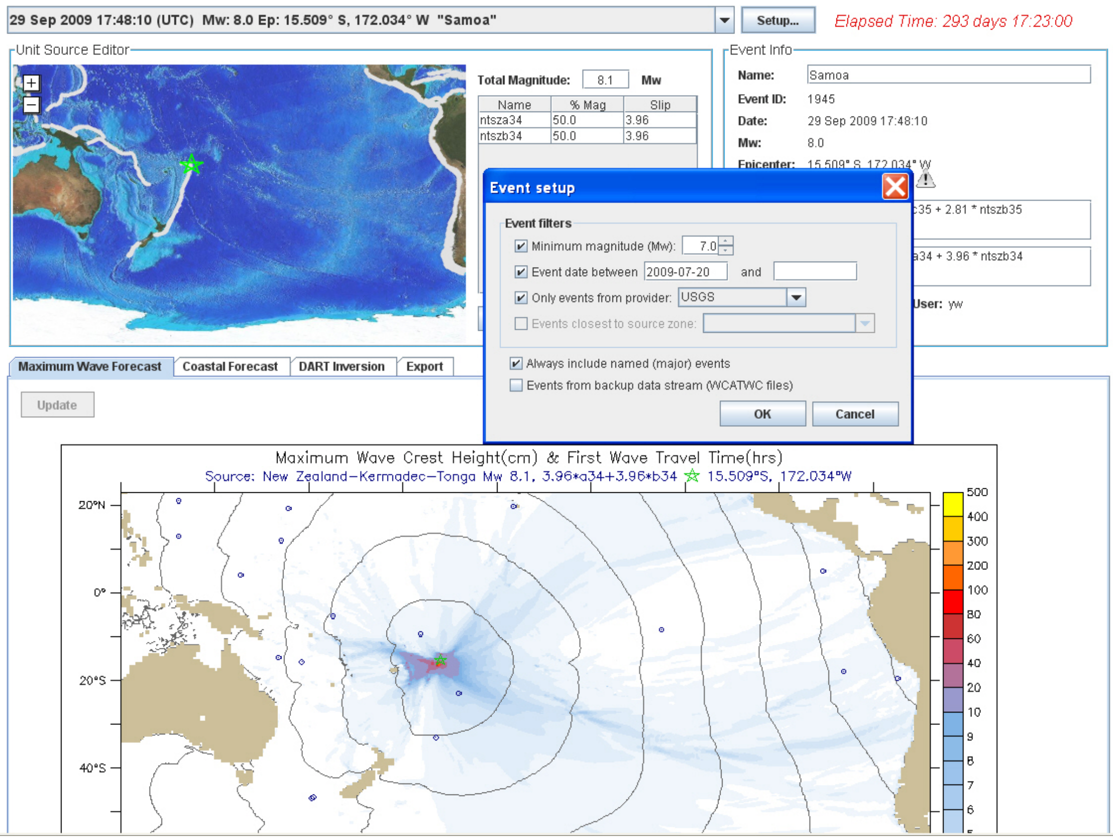

Figure 4.14 User interface of WebSIFT (NCTR, USA) and the forecasted tsunami amplitude and arrival time for the 29 September 2009 Samoa event.

The offshore tsunami wave information, provided by the real-time propagation forecast model, includes variations of wave amplitudes and velocities over time and may be used as an input to other tsunami models to evaluate the nearshore tsunami threat and calculate inundation. To facilitate this procedure, NCTR has also developed a new tool, a web-based Community Modelling Interface for Tsunamis (ComMIT), to provide site-specific inundation forecasts. ComMIT uses the output from a pre-computed tsunami propagation database, i.e., WebSIFT, as the initial condition and has a graphic user interface to output modelled results. ComMIT creates an easy interface between propagation models and inundation models (e.g., inundation modelling in MOST). However, other run-up and inundation models may also be used to simulate inundation process of tsunami with ComMIT.

GDACS (Global Disaster Alert and Coordination System, http://www.gdacs.org/) is another web-based platform for real-time disaster alert and coordination, managed by the European Commission Joint Research Center (Figure 4.15). Different from WebSIFT, GDACS is a cooperative framework that combines existing disaster information management applications. Therefore, it is a “system of systems”. Tsunami is one of the hazards being monitored and evaluated. GDACS can provide near real-time alerts about natural disasters around the world, and it provides real-time access to web-based disaster information systems and related tools to facilitate response coordination, including media monitoring, map catalogues and a Virtual On-Site Operations Coordination Centre.

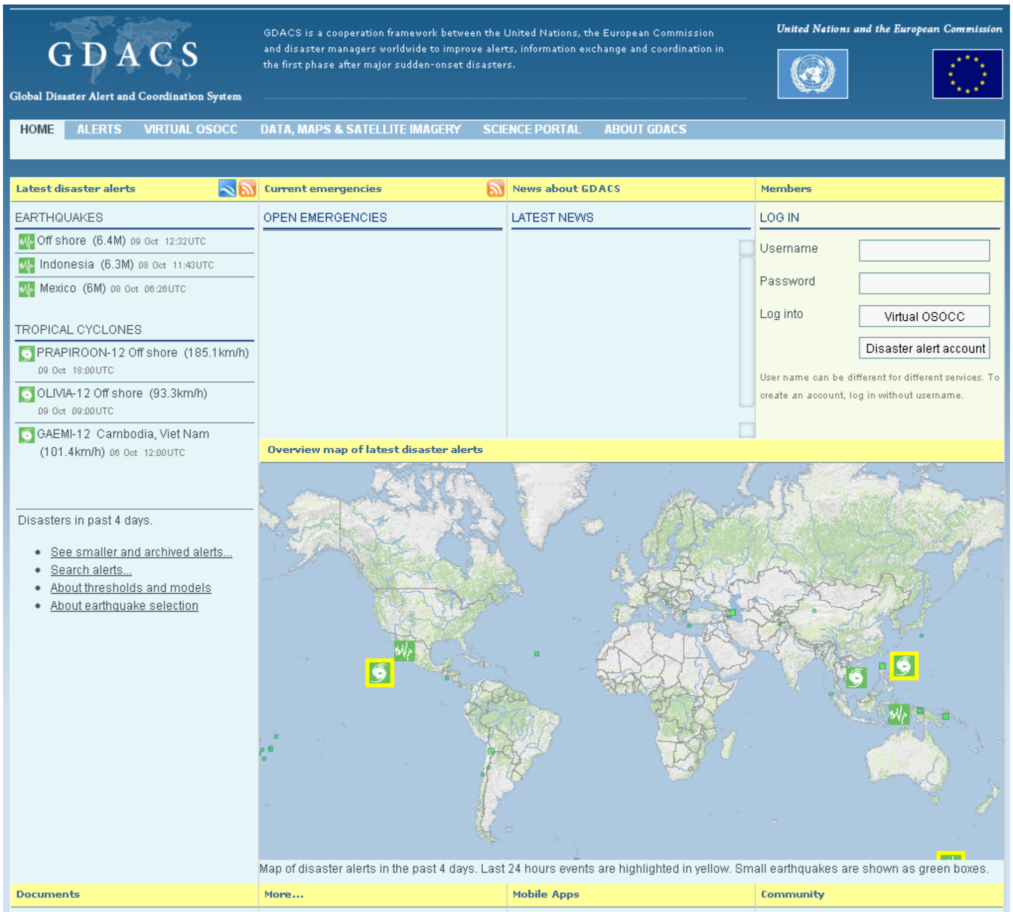

Figure 4.15 Web-based user interface of GDACS (http://www.gdacs.org/).

4.7 PROBLEMS AND LIMITATIONS OF TSUNAMI MODELLING

- In many areas of the world, including New Zealand, data from historical tsunami events, such as wave period, number of waves, inundation depths and extents, and variability along a coast, is very limited. This information is needed to validate models.
- A critical input to propagation models is the bathymetry of the seafloor, especially near-shore bathymetry, which is difficult to obtain but vital to good inundation modelling. This is because the speed, and ultimately the direction, of the tsunami are controlled by the depth of water. Model results are thus only as good as the bathymetry data allow. Much good bathymetry data exists, but combining different sources of bathymetry and processing it into the required form is one of the most labour-intensive aspects of tsunami modelling. Many bathymetry databases are proprietary, and this is also an obstacle to the preparation and use of bathymetry grids for tsunami modelling.
- Most propagation models assume that coastlines behave as perfect reflectors of tsunami waves, but this omits the natural dissipation of tsunami energy which occurs when they run-up against the shore (Dunbar et al., 1989). This leads to a gradual reduction of the accuracy of the model. This is a particular problem for modelling the effect of tsunami from distant sources, as incoming waves may arrive over the course of several hours and interact with earlier waves, especially in locations where tsunami waves may become ‘trapped’ within bays and inlets.
- Inundation modelling requires detailed data on the topography of the areas being considered, ideally with a vertical resolution of less than 0.25 m. Currently, very few areas of New Zealand have topography mapped to this resolution. High-resolution inundation modelling also benefits from data on the size and shape of buildings and on the nature of different land surfaces, e.g. whether forested, cultivated, urban, etc. Ideally the nearshore bathymetry and on-land topography and surface roughness can be obtained as a seamless digital elevation dataset to allow simulations using the full power of high-resolution hydraulic modelling software.
- Characterization of the tsunami source represents the biggest uncertainty for tsunami modelling. Where models are used for real-time forecasting, it is usually possible to determine only very basic information on the characteristics of the source in the time available. This problem also applies to modelling past historical tsunami where little source information may be available. Source details (e.g., slip distribution) are particularly important for local-source tsunami, as they strongly influence run-up. Deep-water wave buoys may be useful in forecasting the potential effects of distant tsunami, as they “record” the source characterization in that particular event and can be used for inverse modelling.

4.8 TSUNAMI MODELLING STUDIES RELEVANT TO NEW ZEALAND

4.8.1 Tsunami modelling studies in New Zealand

Coastal hazard analysis and detailed modelling studies such as maximum tsunami elevations and inundation modelling have been carried out for several regions in New Zealand for tsunami originating from local, regional and/or distant sources. Most of these studies are scenario-based. However, efforts have also been made recently to evaluate tsunami threats probabilistically to account for variations and uncertainties in the sources (e.g., Power et al., 2012; Lane et al., 2012).

The publicly available tsunami modelling and inundation studies are summarized in Appendix 1.

4.9 REFERENCES

Abe, K. (1979). Size of great earthquakes of 1837–1974 inferred from tsunami data. *Journal of Geophysical Research, 84*: 1561-1568.

Abe, K. (1995). Estimate of tsunami run-up heights from earthquake magnitudes. In *Tsunami: Progress in Prediction, Disaster Prevention and Warning*, Adv. Nat. Technol. Hazards Res., vol. 4, Y. Tsuchiya and N. Shuto (eds.), Kluwer Acad.: 21-35.

Abercrombie, R.E.; Antolik, M.; Felzer, K.; Elstrom, G. (2001). The 1994 Java tsunami earthquake: slip over a subducting seamount. *Journal of Geophysical Research, 106(No.B4)*: 6595-6607.

Ammon, C.J.; Kanamori, H.; Lay, T.; Velasco, A.A. (2006). The 17 July 2006 Java tsunami earthquake. *Geophysical Research Letters, 33*, L24308, doi:10.1029/2006GL028005.

Arnold, J.; Carter, J.; Dumas, J.; Gillibrand, P. (2007). Northland Regional Council Tsunami Modelling Study 3. NIWA Client Report: CHC2009-042, June 2009.

Cho, Y.-S. and Yoon, S.B. (1998). A modified leap-frog scheme for linear shallow-water equations. *Coastal Engineering Journal* 40 (2), 191–205.

Dunbar, D., LeBlond, P.H.; Murty, T.S. (1989) Maximum tsunami amplitudes and associated currents on the coast of British Columbia. *Science of Tsunami Hazards 7*: 3-44.

Enet, F.; Grilli, S.T. (2007). Experimental Study of Tsunami Generation by Three-Dimensional Rigid Underwater Landslides. *Journal of Waterway, Port, Coastal and Ocean Engineering, 133(6)*: 442-454.

Enet, F.; Grilli, S.T.; Watts, P. (2003). Laboratory experiments for tsunamis generated by underwater landslides: comparison with numerical modeling. Proc., 13th Offshore and Polar Engineering Conf., ISOPE03, Vol. 3, Honolulu, ISOPE, Cupertino, Calif., 372-379.

Fraser, S.A.; Power, W.L. (2013). Validation of a GIS-based attenuation rule for indicative tsunami evacuation zone mapping. GNS Science Report 2013/02 21 p.

Fritz, H.M. *et al.* (2007). Extreme runup from the 17 July 2006 Java tsunami. *Geophysical Research Letters, 34*, L12602, doi:10.1029/2007GL029404, 2007.

Fryer, G.J.; Watts, P.; Pratson, L.F. (2004). Source of the great tsunami of 1 April 1946: a landslide in the upper Aleutian forearc. *Marine Geology, 203*: 201-218.

Fujii, Y.; Satake, K.; Sakai, S.; Shinohara, M.; Kanazawa, T. (2011). Tsunami source of the 2011 off the Pacific coast of Tohoku Earthquake. *Earth Planets Space, 63*: 815-820.

Geist, E.L. (1998). Local tsunamis and earthquake source parameters. *Advances in Geophysics 39*: 117-209.

Geist, E.L. (2000). Origin of the 17 July 1998 Papua New Guinea Tsunami: Earthquake or Landslide? *Seismological Research Letters, 71(3)*: 344-351.

Gica, E.; Spillane, M.C.; Titov, V.V.; Chamberlin, C.D.; Newman, J.C. (2008). Development of the Forecast Propagation Database for NOAA's Short-Term Inundation Forecast for Tsunamis (SIFT), NOAA Technical Memorandum OAR PMEL-139.

Gillibrand, P.; Arnold, J.; Lane, E.; Roulson, H.; Enright, M. (2011). Modelling Coastal Inundation in Canterbury from a South American Tsunami. Environment Canterbury report number R11/08. ISBN: 978-1-927146-25-5, February 2011.

Goff, J.; Walters, R.; Callaghan, F. (2006). Tsunami source study. NIWA Client Report: CHC2006-082, August 2006.

Heinrich, P. (1992). Nonlinear water waves generated by submarine and aerial landslides. *Journal of Waterway, Port, Coastal, and Ocean Engineering, 118(3)*: 249-266.

Ide, S.; Imamura, F.; Yoshida, Y.; Abe, K. (1993). Source characteristics of the Nicaragua tsunami earthquake of September 2, 1992. *Geophysical Research Letters, 20(9)*: 863-866.

Imamura, F., Shuto, N., Goto, C. (1988). Numerical simulations of the transoceanic propagation of tsunamis. In: Proceedings of the Sixth Congress Asian and Pacific Regional Division, IAHR, Japan, pp. 265–272.

Kajiura, K. (1983). Some statistics related to observed tsunami heights along the coast of Japan, Tsunamis – Their Science and Engineering, Terra Pub., Tokyo, pp. 131-145.

Kanamori, H. (1972). Mechanism of Tsunami Earthquakes. *Physics of the Earth and Planetary Interiors 6*: 346-359.

Kanamori, H.; Kikuchi, M. (1993). The 1992 Nicaragua earthquake: a slow tsunami earthquake associated with subducted sediments. *Nature, 361*: 714-716.

Kennedy, A.B., Chen, Q., Kirby, J.T. and Dalrymple, R.A. (2000). Boussinesq modeling of wave transformation, breaking, and runup. part i: 1d. *Journal of Waterway, Port, Coastal and Ocean Engng*., 126(1):39–47.

Kennedy, A. B., Kirby, J. T., Chen, Q.; Dalrymple, R. A. (2001). Boussinesq-type equations with improved nonlinear behaviour. *Wave Motion* 33, 225–243.

Koshimura, S.; Imamura; F.; Shuto, N. (2001). Characteristics of Tsunamis Propagating over Oceanic Ridges. *Natural Hazards, 24(3)*: 213-229.

Lane, E.; Walters, R.; Arnold, J.; Roulson, H. (2007a). Northland Regional Council Tsunami Modelling Study 1. NIWA Client Report: CHC2007-109. September 2007.

Lane, E.; Walters, R.; Wild, M.; Arnold, J.; Enright, M.; Roulston, H.; Mountjoy, J. (2007b). Otago region hazards management investigation: tsunami modelling study. NIWA Client Report: CHC2007-030. September 2007.

Lane, E.M.; Gillibrand, P.A.; Wang, X.; Power, W. (2012). A Probabilistic Tsunami Hazard Study of the Auckland Region, Part II: Inundation Modelling and Hazard Assessment. *Pure and Applied Geophysics*, DOI: 10.1007/s00024-012-0538-9.

Lavigne, F.; Paris, R., Grancher, D.; Wassmer, P.; Brunstein, D.; Vautier, F.; Leone, F.; Flohic, F.; de Coster, B.; Gunawan, T.; Gomez, C..; Setiawan, A.; Cahyadi, R.; Fachrizal (2009). Reconstruction of tsunami inland propagation on December 26, 2004 in Banda Aceh, Indonesia, through field investigations. *Pure and Applied Geophysics 166(1-2)*: 259-281.

Lay *et al.* (2005). The Great Sumatra-Andaman Earthquake of 26 December 2004. *Science,* 308(5725): 1127-1133, DOI:0.1126/science.1112250

Lay, T.; Ammon, C.J.; Kanamori, H.; Kim, M.J.; Xue, L. (2011a). Outer trench-slope faulting and the 2011 Mw 9.0 off the Pacific coast of Tohoku Earthquake. *Earth Planets Space, 63*: 713-718.

Lay, T.; Yamazaki, Y.; Ammon, C.J.; Cheung, K.F.; Kanamori, H. (2011b). The 2011 Mw 9.0 off the Pacific coast of Tohoku Earthquake: Comparison of deep-water tsunami signals with finite-fault rupture model predictions. *Earth Planets Space, 63*: 797-801.

Liu,P.L.-F., Cho, Y-S., Briggs, M.J., Synolakis, C.E. and Kanoglu, U. (1995). Run-up of solitary waves on a circular island. *Journal of Fluid Mechanics*, 302: 259–285.

Liu, P.L.-F..; Woo, S.-B.; Cho, Y.-S. (1998). Computer programs for tsunami propagation and inundation. Technical report, Cornell University, 1998.

Liu, P.L.-F.; Wu, T.-R.; Raichlen, F.; Synolakis, C.E.; Borrero, J.C. (2005). eRunup and rundown generated by three-dimensional sliding masses. *Journal of Fluid Mechanics, 536*: 107-144.

Lynett, P. and Liu, P. L.-F. (2004a). A Two-Layer Approach to Water Wave Modeling. *Proc. Royal Society of London A*. v. 460, p. 2637-2669.

Lynett, P. and Liu, P. L.-F. (2004b). Linear Analysis of the Multi-Layer Model. *Coastal Engineering*, v. 51(6), p. 439-454.

Madsen, P.A., Sorensen, O.R. (1992). A new form of the Boussinesq equations with improved linear dispersion characteristics: Part II. A slowly varying bathymetry. *Coastal Engineering*, 18, 183–204.

Mansinha, L.; Smylie, D.E. (1971). The displacement fields of inclined faults. *Bulletin of the Seismological Society of America, 61*: 1433-1440.

Mori, N.; Takahashi, T.; Yasuda, T.; Yanagisawa, H. (2011). Survey of 2011 Tohoku earthquake tsunami inundation and run-up. *Geophysical Research Letters, 38*, L00G14, doi:10.1029/2011GL049210, 2011

Nwogu, O. (1993). Alternative form of Boussinesq equations for nearshore wave propagation. J. Waterw. Port Coast. *Ocean Eng.* 119 (6), 618–638.

Okada, M. (1985). Surface deformation due to shear and tensile faults in a half-space. *Bulletin of the Seismological Society of America, 75(4)*: 1135-1154.

Pararas-Carayannis, G. (1992). The tsunami generated from the eruption of the volcano of Santorin in the Bronze Age. *Natural Hazards 5(2)*:115-123.

Pararas-Carayannis, G. (2002). Volcanically Generated Tsunamis. 2nd Tsunami Symposium, Honolulu, Hawaii, USA, May 28-30, 2002.

Pararas-Carayannis, G. (2003). Near and Far-Field Effects of Tsunamis Generated by the Paroxysmal Eruptions, Explosions, Caldera Collapses and Slope Failures of the Krakatau Volcano in Indonesia, on August 26-27, 1883. Presentation for the International Seminar/Workshop on Tsunami "In Memoriam 120 Years Of Krakatau Eruption Tsunami And Lesson Learned From Large Tsunami" August 26-29 2003, Jakarta and Anyer, Indonesia. Also published in 2003 in the *Journal of Tsunami Hazards, Volume 21(4)*: 191-201.

Pararas-Carayannis, G. (2006). Risk Assessment of Tsunami Generation from Active Volcanic Sources in the Eastern Caribbean Region. In *Caribbean Tsunami Hazards* - Proceedings of National Science Foundation Caribbean Tsunami Workshop, March 30-31, 2004, Puerto Rico, Aurelio Mercado-Irizarry and Philip Liu (Eds.), World Scientific Publishing Co. Pte. Ltd., Singapore, 341 pp.

Pedlosky, J. (1979). Geophysical fluid dynamics. Springer-Verlag, 624 pp.

Peregrine, D.H. (1967). Long waves on a beach. *J. Fluid Mech*. 27, 815–827.

Popinet, S. (2003). Gerris: a tree-based adaptive solver for the incompressible Euler equations in complex geometries. *Journal of Computational Physics, 190(2)*: 572-600.

Power, W.L.; Wang, X.; Lane, E.; Gillibrand, P. (2012). A Probabilistic Tsunami Hazard Study of the Auckland Region, Part I: Propagation Modelling and Tsunami Hazard Assessment at the Shoreline. *Pure and Applied Geophysics*, DOI 10.1007/s00024-012-0543-z.

Prasetya, G.; Wang, X.; Palmer, N., Grant, G. (2010a). Tsunami inundation modelling for Tiwai Point. GNS Science consultancy report 2010/293, 75 pp.

Prasetya, G.; Wang, X.; Palmer; N.; Grant, G. (2010b). Tsunami inundation modelling for Riverton and New River Estuary Southland, GNS Science Consultancy Report CR 2011/150, 87 pp.

Satake, K.; Okada, M.; Abe, K. (1988). Tide gauge response to tsunamis: Measurements at 40 tide gauge stations in Japan. *Journal of Marine Research, 46*: 557-571.

Synolakis, C.E.; Bardet, J.-P.; Borrero, J.C.; Davies, H.L.; Okal, E.A.; Silver, E.A.; Sweet, S.; Tappin, D.R. (2002). The slump origin of the 1998 Papua New Guinea tsunami. *Proceedings of the Royal Society of London A 458*: 763-789.

Tappin, D.R.; Watts, P.; Grilli, S.T. (2008). The Papua New Guinea tsunami of 17 July 1998: anatomy of a catastrophic event. *Natural Hazards and Earth System Sciences, 8*: 243-266.

Tappin, D.R.; Watts, P.; McMurtry, G.M.; Lafoy, Y.; Matsumoto, T. (2001). The Sissano, Papua New Guinea tsunami of July 1998—Offshore evidence on the source mechanism. *Marine Geology, 175*: 1-23.

Titov, V.V.; Gonzalez, F.I.; Bernard, E.N.; Eble, M.C.; Mofjeld, H.O.; Newman, J.C.; Venturato, A.J. (2005). Real-Time Tsunami Forecasting: Challenges and Solutions. *Natural Hazards 35*: 41-58.

Tolkova, E.; Power, W.L. (2011). Obtaining natural oscillatory modes of bays and harbors via Empirical Orthogonal Function analysis of tsunami wave fields. *Ocean Dynamics, 61(6)*: 731-751; doi:10.1007/s10236-011-0388-5.

Tsuji, Y.; Imamura, F.; Matsutomi, H.; Synolakis, C.E.; Nanang, P.T.; Jumadi; Harada, S.; Han, S.S.; Arai, K.; Cook, B. (1995). Field survey of the east Java earthquake and tsunami of June 3, 1994. *Pure and Applied Geophysics, 144(3/4)*: 839-854.

Vreugdenhil, C. B. (1994). Numerical Methods for Shallow Water Flow, Boston: Kluwer Academic Publishers, 1994.

Walters, R.A. (1992). A three-dimensional, finite element model for coastal and estuarine circulation. *Continental Shelf Research*, Volume 12, Issue 1, p. 83-102.

Walters, R.A. (2005). Coastal ocean models: Two useful finite element methods. *Continental Shelf Research*, 25:775-793.

Walters, R.A.; Barnes, P.; Lewis, K.; Goff, J.R. (2006). Locally generated tsunami along the Kaikoura coastal margin: Part 2. Submarine landslides. *New Zealand Journal of Marine and Freshwater Research, 40(1)*: 17-28.

Walters, R.A.; Goff, J. (2003). Assessing tsunami hazard along the New Zealand coast. *Science of Tsunami Hazards 21(3)*: 137.

Wang, X.; Liu, P.L.-F. (2007). Numerical simulation of the 2004 Indian Ocean tsunami – Coastal Effects. *Journal of Earthquake and Tsunami, 1(3)*: 273-297.

Wang, X.; Power, W. (2011). COMCOT: a Tsunami Generation Propagation and Run-up Model, GNS Science Report 2011/43, 127 pp., in press.

Wang, X.; Power, W.L.; Bell, R.E.; Downes, G.L.; Holden, C. (2009). Slow rupture of the March 1947 Gisborne earthquake suggested by tsunami modelling. P. 221 In: Barrell, D.J.A.; Tulloch, A.J. (Eds.) Geological Society of New Zealand & New Zealand Geophysical Society Joint Annual Conference, Oamaru, 23-27 November 2009: programme and abstracts. Wellington: Geological Society of New Zealand. Geological Society of New Zealand miscellaneous publication 128A.

Wang, X.; Prasetya, G.; Power, W.L.; Lukovic, B.; Brackley, H.L.; Berryman, K.R. (2009). Gisborne District Council tsunami inundation study. GNS Science consultancy report 2009/233, GNS Science, New Zealand.

Watts, P. (1998). Wavemaker curves for tsunamis generated by underwater landslides. *Journal of Waterway, Port, Coastal, and Ocean Engineering, 124(3)*: 127-137.

Watts, P.; Grilli, S.T.; Tappin, D.R.; Fryer, G.J. (2005). Tsunami generation by submarine mass failure. II: Predictive equations and case studies. *Journal of Waterway, Port, Coastal, and Ocean Engineering, 131(6)*: 298-310.

Wells, D.L.; Coppersmith, K.J. (1994). New Empirical Relationships among Magnitude, Rupture Length, Rupture Width, Rupture Area, and Surface Displacement. *Bulletin of the Seismological Society of America, 84(4)*: 974-1002.

Wijetunge, J.J.; Wang, X.; Liu, P.L.-F. (2008). Indian Ocean tsunami on 26 December 2004: numerical modelling of inundation in three cities on the south coast of Sri Lanka. *Journal of Earthquake and Tsunami, 2(2)*: 133-155.